# Timing and Spectral Properties of Bright Hard GRBs Observed by Suzaku-WAM

Satoshi Sugita[1,2,3], Atsumasa Yoshida[1], Kazutaka Yamaoka[1], Makoto Tashiro[3], Masanori Ohno[4], on behalf of Suzaku/WAM team and HETE-2 team

[1] EcoTopia Science Institute, Nagoya University
[2] Department of Physics and Mathematics, Aoyama Gakuin University
[3] The Institute of Physical and Chemical Research (RIKEN)
[4] Department of Physics, Saitama University
[5] ISAS/JAXA
*E-mail(SS): sugita@u.phys.nagoya-u.ac.jp*

Abstract

We report on a detailed comparison between short GRBs and spikes of long GRBs in timing and spectral properties using bright GRBs observed by Suzaku-WAM. We first performed spectral time lag analysis of 217 spikes in 102 bright GRBs. We found a clear proportional correlation between hard/soft lags and widths of spikes for long GRBs, which is smoothly connected with those of short GRBs. We next performed spike-resolved spectral analysis of 63 spikes for 12 long GRBs with known redshifts, using Suzaku-WAM, Swift-BAT, and HETE-2 data. We found a clear correlation between the intrinsic peak energy ($E_{\rm p}$) and the isotropic radiated luminosity ($L_{\rm iso}$) for individual spikes, $E_{\rm p} \propto {L_{\rm iso}}^{1/2}$, over four orders of magnitude of luminosity. Remarkably, $E_{\rm p}$ and $L_{\rm iso}$ in 6 short GRBs with known redshifts were also within statistical errors of the relation for long GRBs. From these two results, we conclude that, in our sample, there is no clear differences between short GRBs and spikes of long GRBs in the time lag and the $E_{\rm p}$–$L_{\rm iso}$ relation.

Key words: Gamma Ray Burst, WAM, Swift, HETE-2

## 1. Introduction

A Gamma Ray Burst (GRB) is a big explosion in the universe, but the radiation mechanisms are still unknown. It is classified into two subclasses by a duration, *short* (less than 2 sec) GRB and *long* (more than 2 sec) GRB. These subclasses have also differences in other observational properties such as spectral hardness and spectral time lag. Hence they are proposed to have different origin and progenitor (NS-NS or BH-NS merger and collapsar). However, their boundaries are uncertain, and we note that the above properties are obtained from the time-averaged analysis over entire GRB emissions. In fact, many long GRBs have multi-spiked structure with a similar short time scale to that of short GRBs.

To investigate the difference and similarity among short GRBs and individual spikes in long GRBs, we analyzed a large data set from Suzaku/WAM, Swift/BAT and HETE2 data. In this paper, we focus and report on two analysis, the time-lag analysis and time-resolved spectral analysis, for individual spikes, and compare them with short GRB properties.

## 2. Timing Analysis

### 2.1. Spectral Time Lag

The spectral time lag is defined as a peak-time delay between light curves in different energy bands. It is generally known that long GRBs have soft lags in their light curves, while short GRBs show very small lags with less than 0.01 sec(Norris et al. 2006). We calculated the Cross Correlation Function (CCF) and defined a spectral lag $\tau$ as a time difference between zero and a peak of $CCF(\tau)$. Ukwatta et al. (2009) obtained spectral lags by fitting CCFs with the Gaussian profile, but a shape of the CCF in a GRB prompt emission is typically asymmetric around the peak. Hence, in the Gaussian fitting, we need to use only the limited time region around the peak to ignore its asymmetry. To evaluate the peak, we used the following empirical model like log normal distribution to fit the $CCF(\tau)$.

$$N(\tau) = P_1 \times \exp\left[-\frac{(\log(\tau + P_3) - \log(P_4 + P_3))^2}{P_2^2}\right] \quad (1)$$

where $P_4$ is the peak of this function. This model has one additional free parameter to the Gaussian model. We fit the CCFs with the model (1) plus constant value.

### 2.2. Width of Spikes

In order to divide one GRB into several spikes, we assume that a single spike contains only one peak and search for the peaks based on the simple algorithm described in Li & Fenimore (1996). In this method, we define a peak when the time bin satisfies both the following two criteria, a) the count $C_{\rm p}$ at the time $t_{\rm p}$ is the largest in a time range of $t_1 < t_{\rm p} < t_2$, b) $C_{\rm p} - C_{1,2} > N\sqrt{C_{\rm p}}$ for any counts $C_1$ at $t_1$ and $C_2$ at $t_2$ where $N$ is a significance level. Here we set $N$ at 4.

We used Auto Correlation Function (ACF) for time scale estimation of each spike in GRBs. The ACF is a mathematical tool for finding repeating patterns. The width of the ACF indicates a typical time scale of GRB spike. We calculated the ACF and used the Lorentz profile model to fit the $ACF(\tau)$. We define a time scale of GRB spike as the FWHM of the Lorentz-profile of $w_{\rm ACF}$.

### 2.3. Burst Sample and Analysis

For the time lag analysis, we used the WAM BST Time History data which has fine time resolution of 15.625 msec and 4 energy channels (50–100 keV (TH0), 100–250 keV (TH1), 250–500 keV (TH2), >500 keV (TH3)) in the time coverage from $-8$ sec to 56 sec since the trigger. We used all the WAM data from August 17, 2005 to December 31, 2008 for triggered GRBs which were simultaneously detected and confirmed with other satellites. Except for GRBs with bad statistics, 102 GRBs were available for the timing analysis. In this study, we defined short GRBs based on the criteria that $T_{90}$ was less than 2 sec in the 50-5000 keV range. As a result, 20 samples were short GRBs and 82 were long GRBs.

Figure 1 shows $T_{90} - \tau_{02}$ relation where $\tau_{02}$ is the lag measured between TH0 (50–100 keV) and TH2 (250–500 keV) in the $\rm T_{90}$ time region. The distribution between $\tau_{02}$ and $T_{90}$ would have no clear correlation. To evaluate a significance of this correlation, we calculate a Spearman rank-order correlation coefficient $\rho_s$ of the non-parametric method. The correlation coefficient of the $T_{90} - \tau_{02}$ correlation is 0.195 and its chance probability $P_s$ is 0.768. We conclude that there is no correlation between them. In past studies (Norris et al. 2006), short GRBs have lags of less than 0.01 sec. In our results (left panel of Figure 1) we confirmed that short GRBs have short lags, but some of long GRBs with multi-spiked structure showed also short lags of $< 0.01$ sec.

Next, we plot a correlation between spike width $w_{\rm ACF}$ and spectral lag $\tau_{02}$ calculated for each spike (see right panel of Figure 1). The spectral time lag $\tau_{02}$ and each spike width $w_{\rm ACF}$ has a positive and continuous correlation, which just lies on that for spikes of short GRBs. The correlation coefficient of the $\tau_{02}$–$w_{ACF}$ correlation $\rho_{\rm s}$ is 0.783 and its chance probability $P_s$ is less than $10^{-16}$. So this correlation is real at greater than $3\,\sigma$ confidence level. Assuming the correlation, the fitting result with a power law function is $\tau_{02} = (0.12\pm0.02)\times {w_{\rm ACF}}^{1.05\pm0.02}$.

## 3. Time Resolved Spectral Analysis

### 3.1. Burst Sample and Analysis

6 short GRBs (051221, 060801, 061006, 061210, 070714B, and 071227), were simultaneously observed by WAM up to December 31, 2008, We defined the short GRB that the intrinsic duration $T_{90}/(1+{\rm z})$ is less than 2 sec. In case of GRB 070714B, the $T_{90}$ is estimated at 2.562 sec but the $T_{90}/(1+{\rm z})$ of 1.33 sec is less than 2 sec. Hence, we classify GRB 070714B to the short GRB. Table 1 shows observational parameters of the short GRBs. We performed joint fit spectral analysis of the 6 short GRBs with Suzaku-WAM and Swift-BAT

To compare spectral properties among short GRB and spikes of long GRBs, we used 13 bright long GRBs with known redshifts. These are 060814, 061007, 070508, 071003, 080319C which were observed simultaneously by WAM and BAT, 070125 observed by WAM alone, and 020813, 030328, 030329, 041006, 050408, 051022 observed by HETE-2. Table 2 shows observational parameters for 13 long GRBs.

For spike-resolved spectral analysis, we used BST Pulse Height data of WAM, which has 0.5 sec time resolution and 55 energy channels. We derived each time interval of spikes of the GRBs using the peak search algorithm. We extracted the source spectrum from two WAM detectors which detected strong signals from GRBs, and also produced the background spectrum by interpolating the best fit 4th-order polynominal function to the source region when we fit the dead-time-corrected light curves ∼300 s before and ∼300 s after the burst. We calculated the WAM response matrix using the WAM response generator *wamrspgen* (Ohno et al. 2006) version 1.9. The BAT spectra and response matrices were generated for specific time intervals using the standard *Swift*/BAT FTOOLs. We used a response to average the pre-slew, slew and post-slew responses weighted in each interval of the responses since the burst location in the BAT field of view (FOV) changes during the slew. In HETE-2, we used the photon-tagged data of WXM and FREGATE, and accumulated spectra in the standard way. Background spectra were extracted from the time regions before and after GRB source emission intervals. The WXM energy response matrix was calculated for each event using the empirical formula based on the calibration data taken on the ground and in-flight calibrations. The FREGATE response matrix was calculated from extensive Monte Carlo simulations of the detector using GEANT4.

In the previous work of this study, Yoshida et al. (2006) performed spike resolved spectral analysis of the HETE-2 observed GRBs and presented $E_{\rm p}$ - $L_{\rm iso}$ posi-

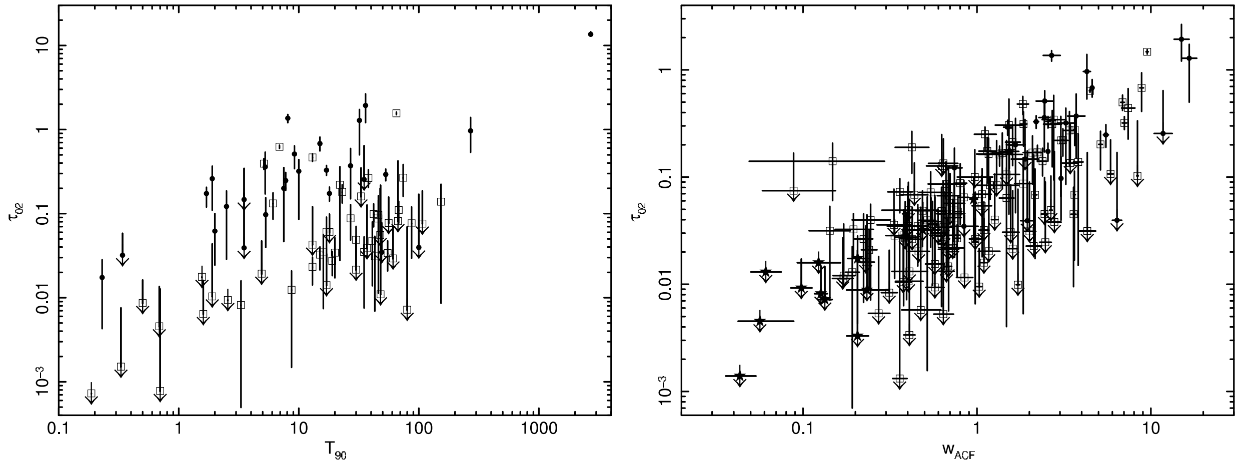


Fig. 1. Left panel: The correlation between duration $T_{90}$ (s) and spectral lag $\tau_{02}$ (s) calculated in entire emission region, where circle points are single spiked GRBs and square points are multi spiked GRBs. Right panel: The correlation between spike width $w_{\rm ACF}$ (s) and spectral lag $\tau_{02}$ (s) calculated in each spike. Filled circle points are the spikes of Single spike bursts, filled square points are the spikes of Multi-spike bursts and filled star points are the spikes of short GRBs, which have a Spearman rank-order correlation coefficient $\rho_{\rm s}$ = 0.783 and significance probability $P_{\rm s} < 10^{-16}$. The fitting result with single power-law model is $\tau_{02} = (0.12 \pm 0.02) \times w_{\rm ACF}{}^{1.05\pm0.02}$.

tive correlation of the the spikes. In this study, we plot all the 63 points of $E_{\rm p}$ - $L_{\rm iso}$ of 12 multi spike GRBs. The left panel of Figure 2 shows that $E_{\rm p}$ - $L_{\rm iso}$ correlation of the all spikes have a positive correlation which spans four-order Luminosity. To test the significance of the correlation, we calculate the Spearman rank-order correlation coefficients. We obtain the correlation coefficients 0.87 for $E_{\rm p}$ - $L_{\rm iso}$ correlation of the all spikes, and the chance probability that there is no correlation of $< 10^{-16}$. Assuming the correlation between $E_{\rm p}$ - $L_{\rm iso}$, we fit the correlation with $E_{\rm p} = (543 \pm 10) \times L_{\rm iso,52}{}^{0.51\pm0.01}$. The dispersion of distance from the best fit of the points is 1 $\sigma \sim 0.26$, assuming the Gaussian distribution.

For comparison with spikes of long GRB, we performed spectral analysis of 6 redshift-known short GRBs. We plot the points of 6 short GRBs on the $E_{\rm p}$ - $L_{\rm iso}$ correlation for all the spikes (right panel of Figure 2). It shows that $E_{\rm p}$ - $L_{\rm iso}$ points of 6 short GRBs are consistent with this correlation within 3 $\sigma$.

Table 1. Sample of redshift-known short GRB by WAM and BAT.

| GRB | $T_{90}/(1+{\rm z})^1$ | z | Instruments |
|---|---|---|---|
| 051221 | 0.121 | 0.5465 | BAT, WAM1+2 |
| 060801 | 0.191 | 1.131 | BAT, WAM0+3 |
| 061006 | 0.261 | 0.4377 | BAT, WAM3 |
| 061210 | 0.033 | 0.4095 | BAT, WAM2+3 |
| 070714B | 1.334 | 0.92 | BAT, WAM0+3 |
| 071227 | 1.129 | 0.383 | BAT, WAM3 |

*1 We defined the short GRB with the criteria that the intrinsic duration $T_{90}/(1+{\rm z})$ is less than 2 sec.

Table 2. Sample of spike resolved spectral analysis by WAM, BAT and HETE-2.

| GRB | $T_{90}/(1+{\rm z})^1$ | z | Instruments |
|---|---|---|---|
| 060814 | 40 | 0.84 | BAT, WAM0+2 |
| 061007 | 24 | 1.261 | BAT, WAM2+3 |
| 070125 | 16 | 1.547 | WAM1+2 |
| 070508 | 7 | 0.84 | BAT, WAM1+2 |
| 071003 | 10 | 1.60345 | BAT, WAM1+2 |
| 080319C | 4 | 1.95 | BAT, WAM2+3 |
| 020813 | 54 | 1.25 | HETE-2 |
| 030328 | 40 | 1.52 | HETE-2 |
| 030329 | 33 | 0.168 | HETE-2 |
| 041006 | 22 | 0.716 | HETE-2 |
| 050408 | 15 | 1.2357 | HETE-2 |
| 051022 | 99 | 0.8 | HETE-2 |

## 4. Discussion and Conclusion

We found no correlation between the lag and the duration for GRB entire emissions, while there is a clear correlation between the lag and the width for spikes of long GRBs. This means that the lag depends on not overall structure but individual spike that is responsible for each internal shock among baryon shells. It is consistent with the the theoretical model that the time delay between different energy bands is due to the time difference between the emission to a line of sight and the emission with respect to high-latitude in conical jet structure (Ioka & Nakamura 2000). For short GRBs, we could not find any clear difference with long GRBs in a correlation between the lag and the width.

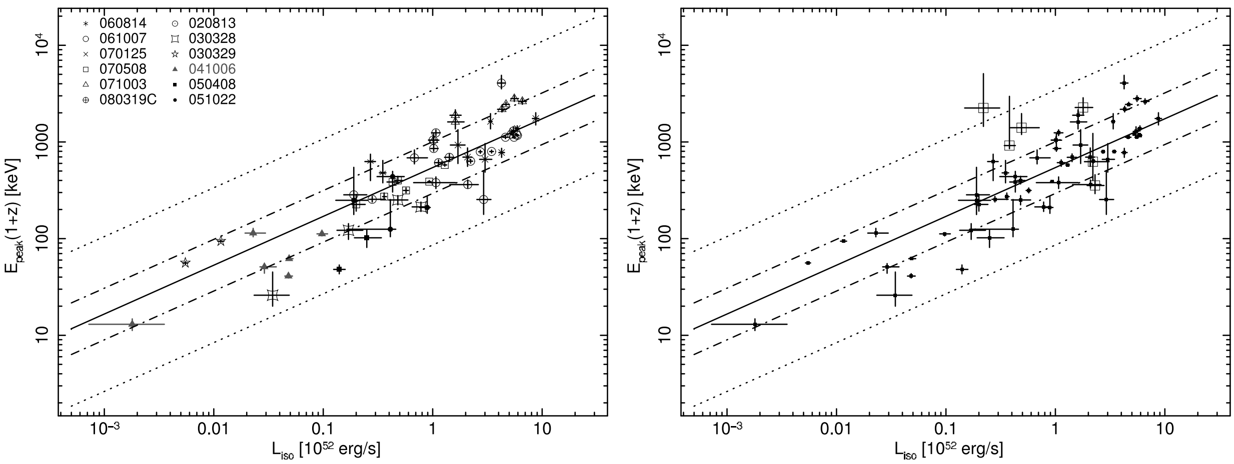


Fig. 2. Left panel: $E_{\mathrm{p,i}}$–$L_{\mathrm{iso}}$ plane of the 63 spikes of 12 multi spike GRBs. The continuous line is the best fit to the sample with a power-law as $E_{\mathrm{p}} = (543 \pm 10) \times L_{\mathrm{iso},52}{}^{0.51\pm0.01}$. dash-dotted lines are 1 $\sigma$ errors and dotted lines are 3 $\sigma$ errors. Right panel: $E_{\mathrm{p,i}}$–$L_{\mathrm{iso}}$ correlation of the long GRB spikes and 6 short GRBs. Open square points are short and closed square points is long GRB Spikes. The continuous line is the best fit to the sample of the long GRB spikes with a power-law model.

In the spike-resolved spectral analysis, we found the $E_{\mathrm{p}} - L_{\mathrm{iso}}$ correlation as $E_{\mathrm{p}} \propto L_{\mathrm{iso}}{}^{0.51\pm0.01}$. According to the synchrotron shock model (Zhang & Mészáros 2002), the peak energy $E_{\mathrm{p}}$ is considered to be the typical synchrotron energy $\gamma_{\mathrm{m}} m_{\mathrm{e}} c^2$ and the relationship between the $E_{\mathrm{p}}$ and the luminosity $L_{\mathrm{iso}}$ can be derived as $E_{\mathrm{p}} \propto r^{-1} L_{\mathrm{iso}}{}^{0.5}$, where $r$ is a radius of the emission region. Our derived correlation is fully consistent with one expected from the synchrotron shock model. The slope is always constant for each spike, suggesting that the $r$ is constant. It implies that each spike corresponds to the synchrotron emissions from accelerated electrons in each internal shock, which takes place at roughly the same distance $r$. Moreover, at least 6 short GRBs with known redshifts are satisfied with the correlation.

In our time lag analysis and spectral analysis using the Suzaku WAM data, we could not see any clear difference between short GRBs and spikes of long GRBs. This means that some short GRBs might have similar characteristics and also similar progenitors to long GRBs in the classical classification based on the duration.

## References

Hakkila, J. et al. 2008 ApJ, 677, 81
Li, H. & Fenimore E. E. 1996, ApJ, 469 L115
Norris, J. P. & Bonnell, J. T. 2006 ApJ, 643, 266
Ohno, M. et al. 2005 IEEE Trans. Nucl. Sci., 52, 2758
Ohno, M. et al. 2009 PASJ, 61, 201
Ukwatta, T. N. et al. 2009 arXiv0908.2370U
Yamaoka, K. et al. 2009 PASJ, 61, S35
Yoshida, A. et al. 2006 NCimB, 121, 1267
Zhang & Mészáros 2002 ApJ, 581, 1236